Functionalization of Poly-(ethylene glycol)-diacrylate (PEGda) with different molecular mass using Two-Photon-Polymerisation

Internship at

Fraunhofer Insitut für Werkstoff und Strahltechnik

Dresden

April - June 2014

Diederik van Lith

Internship Report

Diederik van Lith
(s0143677)

Student of

Twente University

Faculty of Engineering Technology
Chair of Applied Laser Technology

Enschede, The Netherlands

Supervisor

Dr.ir. G.R.B.E. (Gert-Willem) Römer

Assignment at

Fraunhofer Institut für Werkstoff und Strahltechnik
Department of Surface Functionalization

Dresden, Germany

Supervisor

Dipl.-Ing. M. (Matthias) Bieda

During the period

April 2014 – June 2104

Index

1 Introduction

Production processes that enable ever smaller scale features to be created have driven technological advancement in the past decades. From the creation of the first microprocessor until the smart-phones available today, the possibility to create smaller and smaller features has been of utmost importance. As a relatively new production process Two-photon-polymerization, (2PP) is a promising process to produce free form 3D structures directly, without the use of masks or building layer after layer involving the repetition of different process steps like some other lithographic processes require. Besides the practical benefit of not involving several process steps, another great advantage of 2PP is that it enables the fabrication of very small features down to even 30 nm (Juodkazis et al. 2005). Moreover the process is suited for a large variety of different materials and thus suited for applications in a lot of different fields like micro scale optical components (Hiroaki Nishiyama, Yoshinori Hirata, book - Lithography 2010), or the replacement of inner ear bones (Ovsianikov et al. 2007).

The current work will focus on the processing of Poly (Ethylene Glycol) diacrylate (PEGda) a biocompatible material that, among other medical applications, is used in tissue engineering to produce scaffolds that support the growth of cells into 3D tissues. Besides it´s relatively low cytotoxicity another main advantage of using PEGda as precursor is the availability of PEGda of different molecular masses, each resulting in different mechanical properties of the polymer that is obtained after processing.

The final goal is to produce a hollow fibre to be used in a lab-on-a-chip system. The fibre will provide cell cultures with the necessary nutrients. And will be in direct contact with the cells. An earlier effort to create a hollow fibre out of Ormocomp was made. Ormocomp is a commercially available resin to be used for 2PP. An important requirement of such a fibre however, is that it should not be toxic to the cells in question. So biocompatibility of the materials used is definitely of importance. The biocompatibility of PEGda is better than that of Ormocomp and moreover, structures out of PEGda are biodegradable and are absorbed by living tissue over time. In order to do further research into the possibilities that 2PP of PEGda has to offer, it is important to get a picture of how different parameters (e.g. laser power, writing speed, different photo initiators and water content) are of influence on results of the polymerization process. The current focus will be specifically on getting a picture of the process window of PEGda 600, PEGda 700 and PEGda 3460 with the photo initiators Irgacure 2959 and Irgarcure 369.

In the first chapter, the process of Two Photon Polymerization will be explained as well as the material under investigation and a few of its implementations. The second chapter describes the goal of the current research, the experiments that were done as well as the materials that were used and the procedures that were followed. The results of the experiments can be found in the third chapter. Subsequently the conclusions that can be made from these results will be explained in the fourth chapter and finally a short discussion about the work presented here and an outlook on further research will be given.

2 Fundamentals

Before the experiments and their results will be discussed it is essential to have an understanding of the process of 2PP and the materials that were used. In this chapter the process of 2PP and the properties of PEGda and the photo initiator (Irgacure) will be explained.

2.1 Two Photon Polymerization

Two-photon polymerization is a process in which a polymerization reaction is triggered by the simultaneous absorption of two photons, so called two photon absorption, 2PA. The existence of the process of an atom simultaneously absorbing two photons to reach its aggregated state was already predicted by M. Göppert Mayer (Göppert-Mayer 1931). The means of causing this phenomenon to occur however were not available until the first LASER devices came around. In 1961 2PP was demonstrated in practice for the first time (Kaiser, Garrett 1961).

In two photon absorption, a so-called virtual intermediate state is involved (see Figure 1). The first photon excites an electron up to this virtual intermediate state and a second photon can be absorbed to bring the electron into an excited state as long as the virtual intermediate state has not decayed. This virtual intermediate state only exists for a period in the order of 1 – 10 femtoseconds (Birge, Pierce 1986).

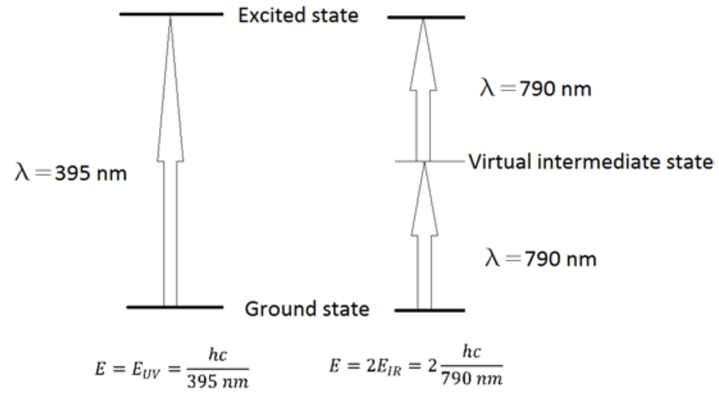

Figure 1 One photon absorption versus two photon absorption

As one can imagine, the density of photons passing through the material needs to be immensely high in order for two photons to be absorbed within this period of time. The photon density required to achieve this is far beyond the capabilities of any conventional light source. With modern ultra-short pulsed lasers however, this energy density can be obtained.

Because the excited state in 2PA is reached by absorbing two photons, the rate of 2PA is proportional to the square of the local power intensity. Furthermore the photochemical reaction that is involved in initiating the polymerization process shows a certain threshold effect with respect to the radiation intensity. As explained before, the number of photons passing through the material needs to be very high in order for 2PA to occur. Because of this quadratic relation and this threshold effect, the process of 2PA can be easily confined to the focus spot of the beam, whereas One photon absorption, which is directly proportional to the local power intensity, will occur along the full length of the beams path through the resin.

Another benefit of this threshold effect is that 2PP does not occur over the entire waist diameter of the beam. It only occurs in the area where the power intensity exceeds the threshold value. While the minimum waist size is limited to the diffraction limit, the minimum feature size can be smaller than that due to this threshold effect. Therefore the 2PP process is perfectly suited to write very small details and by manipulating the location of the focus relative to the work piece, three dimensional structures can be created.

2.2 PEGda and its Applications

Polymers, such as PEGda, are materials that are made up of very long molecules with typically a chain of carbon atoms as a backbone. These long molecules are fabricated by connecting a series of smaller molecules (monomers) or groups of these smaller molecules (oligomers) together. Typically the way to bond these small molecules together is to break up unsaturated carbon bonds in the monomer molecules, which creates a chain reaction of monomers forming a long chain. To get this chain reaction started in photo polymerization, a so called photo-initiator is used. The photo-initiator is sensitive to light and upon absorption of a photon, forms radicals which are able to break up the unsaturated bonds in the monomer and bind themselves to them, resulting in a monomer radical with the photo-initiator molecule attached to it. This newly formed radical in turn can break up another saturated bond and attach itself to a second monomer. This process results in a chain reaction until two radicals meet up and form a completed chain.

One of the characteristics of PEGda is that different types of cells are able to survive on surfaces and structures made out of PEGda, it is bio-compatible. PEGda has been used for a number of different applications in bio- and tissue engineering. Some examples of such applications are the building of scaffolds for tissue engineered heart valves (Durst et al. 2011) or the creation of PEGda particles containing cells (Panda et al. 2008) for different tissue engineering or drug delivering purposes.

2.3 Energy Absorption

As mentioned earlier, the 2PP-process shows a certain threshold with respect to the energy needed to initiate the process. The energy absorbed by the photo initiator can be taken as a measure to quantify the 2PP-process and give a theoretical basis to the influence of the process parameters. Following the same procedure as Pruzinsky et. al. (Pruzinsky, Braun 2005), the energy absorbed per cubic centimeter by the photo initiator by means of 2PA can be calculated. In order to do that, first the waist diameter of the focused beam and the number density of the photo initiator in the different resins need to be calculated.

As not all data of the optics used in the experimental setup and the diameter of the laser beam are available, some assumptions had to be made in calculating the waist diameter of the focused beam. First of all, it was assumed that the focusing optics are perfect (i.e. aberration free) and secondly the unfocussed beam diameter at the receiving end of the objective was assumed to be equal to the diameter of the focusing objective. This allows a rough approximation of the beams waist diameter with the following expression (Dr. ir. G.R.B.E. Römer 2009):

$$d = \frac{4M^2}{\pi}\frac{\lambda f}{D} = \frac{4M^2}{\pi}\frac{\lambda}{2N.A.}$$

Parameter	Meaning	Value (units)
d	Waist diameter	0.629 (μm)
M^2	Beam quality	1.00 (-)
λ	Wave length	790 (nm)
f	Focal length	unknown (m)
D	Unfocussed beam diameter	c.a. 7.8 (mm)
$N.A.$	Numerical Aperture	0.8 (-)

Table 1 Description of parameters in calculating focus diameter

Secondly the number density, i.e. the number of molecules per cubic meter, of the photo initiator has to be calculated. Given the composition of the different mixtures in Appendix 1, the number density of the photo initiator can be calculated as follows:

$$N_i = \frac{m_{pi}N_A}{M_{pi}V_{tot}} \qquad V_{tot} \approx \frac{m_{tot}}{\rho_{PEGda}}$$

Parameter	Meaning	Value (units)
N_i	Number density	To be calculated (cm^{-3})
m_{pi}	Mass Photo initiator	- (g)

N_A	Avogadro constant	$6.022 \cdot 10^{23}$ (-)
M_{pi}	Molar mass photo initiator	366.5 (g/mol)
m_{tot}	Total mass	- (g)
ρ_{PEGda}	Density of PEGda	1.12 (g/ml)

Table 2 Description of parameters in calculating number density

Since the mixtures consist of r 99%$^{wt.}$ and 99.5%$^{wt.}$ PEGda 700 respectively, the amount of photo initiator is neglected in calculating the total volume of the mixture. Based upon the data in Appendix 1, the number density was calculated to be $1.885 \cdot 10^{13}$ cm^{-3} for the mixture with 1%^{wt} Irgacure 369 and $8.891 \cdot 10^{12}$ for the mixture with 0.5 %$^{wt.}$ Irgacure 369.

Finally the energy absorption of the photo initiator can be calculated:

$$E = \tau_{exp} N_i \frac{\sigma_{TPA}}{h\omega} \frac{4}{\pi^2 d^4} \frac{g_p}{\tau_p F} < P(t) >^2 \qquad \tau_{exp} = \frac{v}{d}$$

Parameter	Meaning	Value (units)
E	Absorbed Energy	To be calculated (J/cm^3)
τ_{exp}	Exposure time (s)	- (s)
v	Writing speed	- (μm/s)
d	Waist diameter focused beam	0.629 (μm)
N_i	Number density op P.I.	- (cm^{-3})
σ_{TPA}	TPA cross section (Schafer et al. 2004)	$4 \cdot 10^{-51}$ (cm^4 s photon^{-1})
g_p	Dimensionless factor for pulse shape(Xu, Webb 1996)	0.664 (-)
τ_p	Pulse duration	73·fs
F	Repetition rate	73.1 (MHz)
$h\omega$	Energy per photon	$2.51 \cdot 10^{-19}$ (J)
$< P(t) >$	Time averaged Power	- (W)

Table 3 Parameters of influence on the absorbed energy by 2PP

With the assumption that the exposure time can be approximated by dividing the waist diameter of the beam by the writing speed, the formula can be used to calculate the absorbed energy in the case of continuous writing instead of creating single voxels with a fixed exposure time. In this formula the fact that every pulse lands on a slightly different position due to the fact that the sample is moving, is not taken into account. A more accurate calculation could be made by incorporating this into the calculation.

This formula enables the calculation the amount of energy absorbed as function of the laser power and the writing speed. Later on in chapter 4, the amount of energy absorbed by the resin due to 2PP will be compared to the results of the experiments.

3 Experimental

In this part the goal of the experiments as well as the properties of the experimental set up, the design of the experiment and the procedures that were followed will be described.

3.1 Materials

To get a good understanding of the experiments and the meaning of the results, the precursor and photo initiators that were used are described in this section.

3.1.1 Precursor

Different types of PEGda were used, all differing in molecular mass, see Figure 2. The unsaturated bonds at the both ends of the carbon chain are involved in the polymerization reaction as described in paragraph 2.2. The middle part, denoted with 'n' can be varied in length to create PEGda with an different molecular mass. This part of the molecule does not take part in the polymerization reaction, so by changing the molecular mass of the PEGda the crosslink density of the resulting polymer is also changed. This changes the mechanical properties of the polymer significantly. In the current work PEGda 3460, PEGda 700 and PEGda 600 were used. PEGda3460 is a almost white powder at room temperature, while PEGda 700 is a solidified gel at 6°C and a liquid at room temperature. PEGda 600 is stored at room temperature in liquid state.

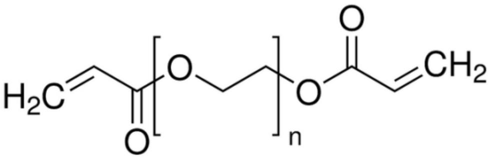

Figure 2 Chemical makeup of PEGda of arbitrary molecular mass.

3.1.2 Photo Initiator

Irgacure 369, supplied by BASF, is one of the photo initiators used. In Figure 3 the extinction spectrum of Irgacure 369 is shown, which is directly related to the absorption spectrum. Depending on the concentration of Irgacure 369 in the resin, it will absorb a certain amount of light between wavelengths of 200 nm up to a little more than 425 nm. In this case a 790 nm Titanium:Sapphire laser was used. At his wavelength the photo initiator will not absorb any photons. When the light intensity reaches a certain threshold however, 2PA can occur in which case two 790 nm photons will be absorbed simultaneously as if it were 395 nm photons. As can be seen in the absorption spectrum, at this wavelength Irgacure 369 does absorb photons.

Irgacure 2959 however, has a different extinction spectrum and as can be seen in Figure 4, it does not absorb any light at a wavelength of 395 nm. This means that Irgacure 2959 is not suited to be used as a photo initiator when working with a wave length of 790 nm.

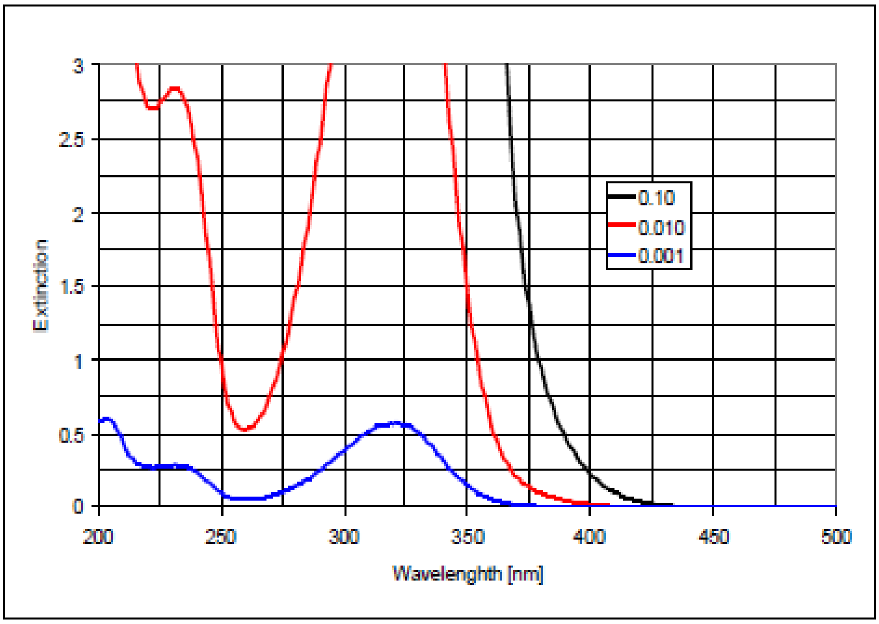

Figure 3 Extinction spectrum of Irgacure 369 (Ciba Specialty Chemicals Inc 2001a)

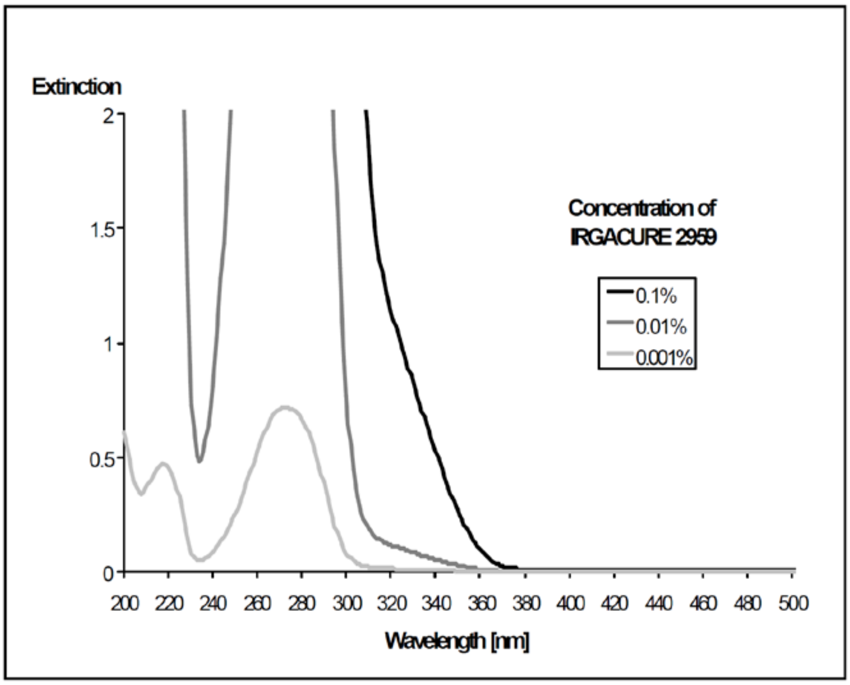

Figure 4 Extinction spectrum of Irgacure 2959 (Ciba Specialty Chemicals Inc 2001b)

3.2 Preparation of mixtures

As only a small amount of resin is required for each experiment, small quantities of the different resins were prepared. To calculate the required amount of different substances the goal was set to produce 3 grams of resin in total. The required amount of photo initiator and precursor can be easily calculated by multiplying the desired mass fraction by this total amount of resin to be produced. An overview of the actual composition of the produced resins can be found in Appendix 1 on page 21.

In general fluids were handled using a pipette, which enables careful dosing. Solids were handled using a metal scope. The amounts of both liquids and fluids were measured using a scale. PEGda 700 however is a different case since it is solid at 6˚C, it is stored in the fridge, and liquid at room temperature. The most practical way to handle it was by using a metal scoop to put the desired amount in to a plastic tray in order to weigh it on the scale and then pouring it into a glass bottle to mix it with the rest of the components, any bits left behind in the plastic tray were carefully scraped into the glass bottle.

After preparing the resins, they were shielded from light and stored at room temperature.

3.3 Preperation of Samples

An object glass was used to build the sample on as shown in Figure 5. First, two small drops of water were placed at both ends of the glass in order to keep the spacers in place. On top of both droplets a spacer was placed and again a small droplet of water was deposited on each spacer. After that a drop of the mixture to be used (c.a. 0.1 mL) was deposited on the substrate using a syringe. Finally a cover glass was carefully placed on top in such a way that no bubbles would form in the mixture.

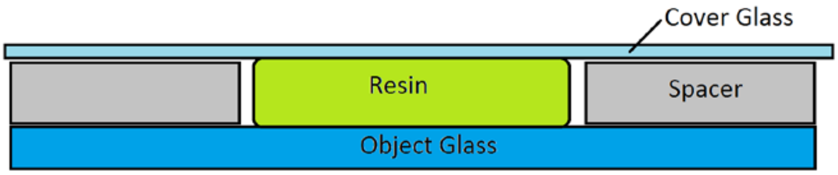

Figure 5 Schematic of sample layout

3.4 Development

After the writing process the sample was put in a petri dish and two weights were placed on the cover glass at the location of the spacers to prevent the surface tension of the water from removing the cover glass in an uncontrolled fashion. The petri dish was filled with deionized water up to the point where the sample was completely submerged. After a period of 10 minutes the weights, the cover glass and the spacers were carefully removed, while taking care that no damage was done to the produced structures. The sample was left in the water bath for another 10 minutes, in order to allow the remaining bulk of unexposed precursor to dissolve into the water. Finally the sample was taken from the petri dish and the water was drained from the sample by keeping it in a vertical position for up to 30 seconds. Any water remaining on the sample was carefully blown away with air.

3.5 Experimental Set-up

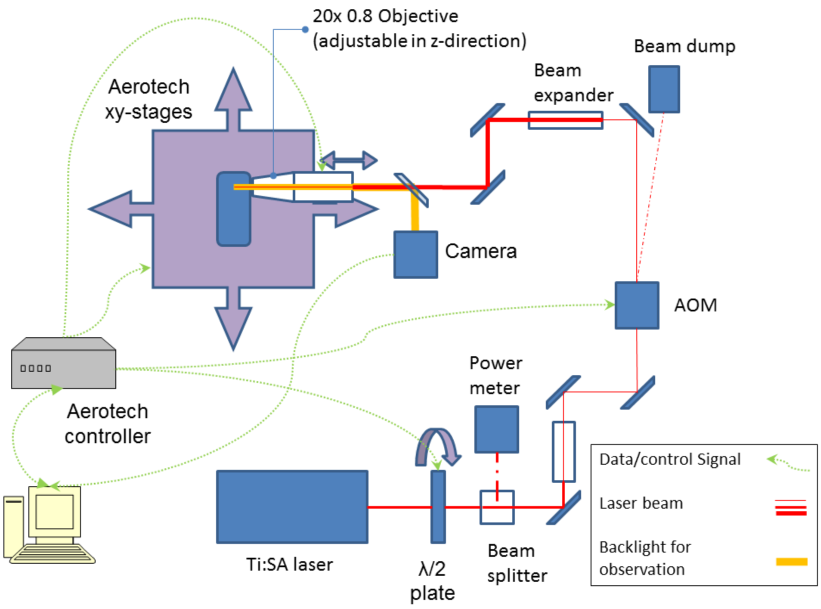

Figure 6 Schematic of the laser setup

In Figure 6 a schematic overview of the experimental set-up is presented. When following the path of the beam, starting at the source, the beam passes through a half-wave-plate which is used to manipulate the polarization of the beam. In combination with the beam splitter, which splits the beam depending on its polarization, the laser power reaching the sample can be manipulated. After the beam splitter the laser beam is tightened, because the AOM can only fit a beam with a maximum diameter of 1.3 mm. The Acoustic Optic Modulator works like a grating and, when activated, diverts the 1st diffraction of the beam further along the path to the sample. If the AOM is not active, the beam ends in the beam dump. So practically the AOM works as a remote controlled shutter enabling the beam to passed or blocked by Aerotech controller. After the AOM, the beam passes trhough a beam expander to expand the beam diameter (a bigger diameter results in a smaller focus spot) and to collimate it. Finally the beam passes a focusing objective with a magnification of 20x and a numerical aperture of 0.8, which focusses the beam on the sample.

To enable 3D writing the ability to move the laser focus spot in x-, y- and z-direction relative to the sample is required. Movement in the horizontal plane (i.e. x and y direction) are realized by mounting the sample on and XY-stage. The movement in vertical direction is realized by moving the focusing objective in Z-direction.

Property	**Measured Value (units)**
Time average power	520 (mW)
Pulse duration	72 (fs)
Pulse Frequency	73.1 (MHz)
Pulse Energy	6.9 (nJ)
M^2	X: 1.00 Y:1.01

Table 4 Properties of the femtosecond laser source

The laser power reaching the sample cannot be measured directly due to the very small working distance of the focusing objective. However the power of the beam at a point right before the focusing objective is known. A graph provided by the manufacturer of the objective shows that the transmittance of light at a wavelength of 790 nm is approximately 0.9. Taking this 10% loss of power into account the laser power reaching the sample is estimated to be as shown in Figure 7.

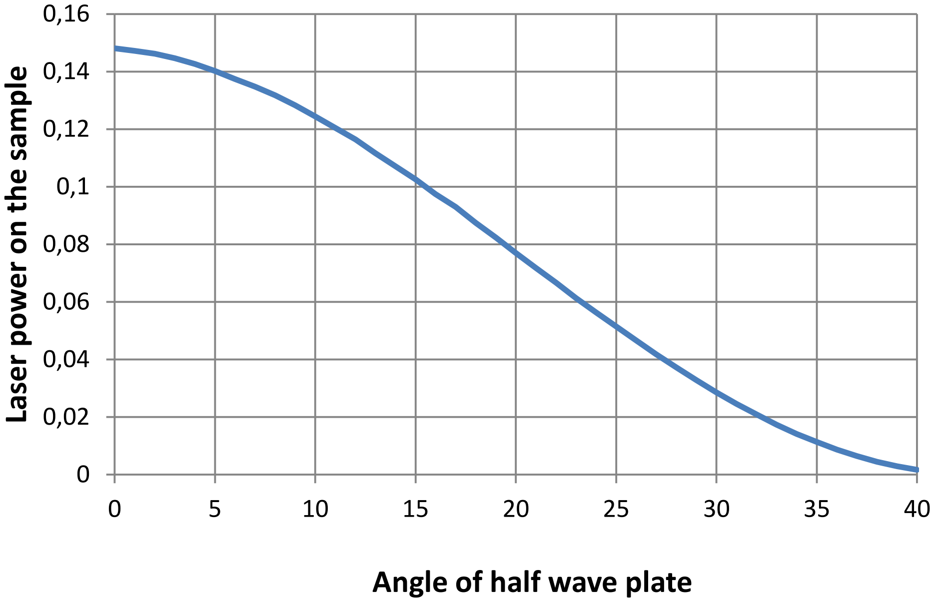

Figure 7 Laser power at the sample as function of the half-wave-plate angle

3.5.1 Improvement of mechanical performance

During the writing process it is important that the velocity at which the sample moves relative to the laser focus is constant, to get a constant and homogenous structure. In earlier experiments with Ormocomp, a problem with over polymerization was observed at the beginning of writing a line. The problem seemed to be originating from the fact that the system needs a little time to accelerate up to the desired speed. In this period of time the actual speed is lower, which can result in over polymerization.

Moreover, the air bearings of the Y-stage have proven to be a problem when large accelerations in X-direction are applied. The air pressure in the gap between the stage and its guiding rail is not enough to counter the perpendicular force resulting from the acceleration in X-direction, and thus the Y-stage bumps into its guiding rail.

To prevent the Y-stage bumping into the guiding rail, the maximum acceleration in X-direction was lowered. First of all this was achieved by changing the motion profile from the default sine ramp into the Aerotech supplied SCURVE, which according to the documentation has a lower peak acceleration value. Moreover using some G-code commands (G65 and G66) the maximum acceleration and deceleration values can be specified.

These measures however make the problem of having a too low velocity at the beginning of writing each line even bigger. To solve this problem, an extra piece of trajectory was programmed to bring the system up to speed before turning on the laser. During this piece of trajectory, the stage accelerates to the desired speed and travels at a constant speed until it reaches the beginning of the line to be written, where the laser is switched on. After writing the desired length, the laser is switched off and the system uses some time to gently decelerate and get into position for the next line to be written.

As a last improvement of the mechanical performance of the stages, the crossover frequency, F_c, was increased by changing the controller settings. Simply put, a closed loop mechatronic system, like the Aerotech stages, works like a low-pass filter. The input of the filter is the desired motion profile and the output is the realized motion. The cross over frequency is the frequency at which the input signal is cut off. By increasing F_c the realized motion will look more like the desired motion profile since less of its frequency content is filtered out. The effect of increasing the crossover frequency can be seen in Figure 8. To indicate when the laser is on, the scaled output signal to the AOM was also plotted. When the signal is high, the laser is on and the velocity error should be minimal. Both plots were generated using the extra trajectory to get up to speed and a maximum speed of 20 mm/s.

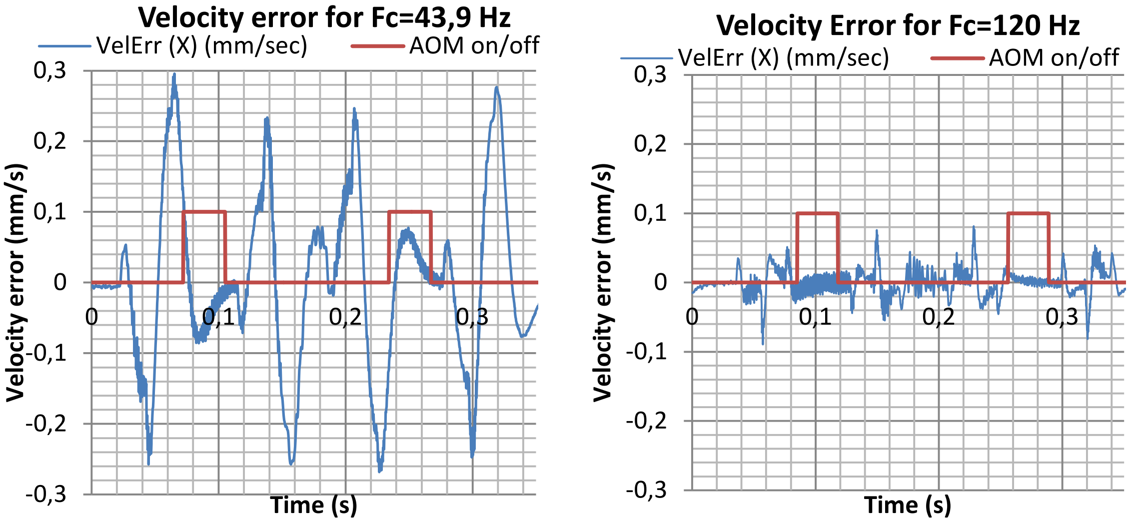

Figure 8 Reduction of velocity error by increasing crossover frequency.

3.6 Design of Experiment

In order to investigate the influence of laser power and writing speed on the two photon polymerization process, matrices of small squares with varying writing speed and laser power were produced see Figure 9. The dimensions of each square are 15 µm by 15 µm. The squares consist of lines in the direction of the velocity axis with a spacing of 0.7 µm. The power was varied with constant steps in the angle of the half-wave-plate and since the relation between the power and the half-wave-plate angle is not linear see Figure 7, the power difference between two adjacent squares in the matrix is not constant. The speed was changed with constant steps.

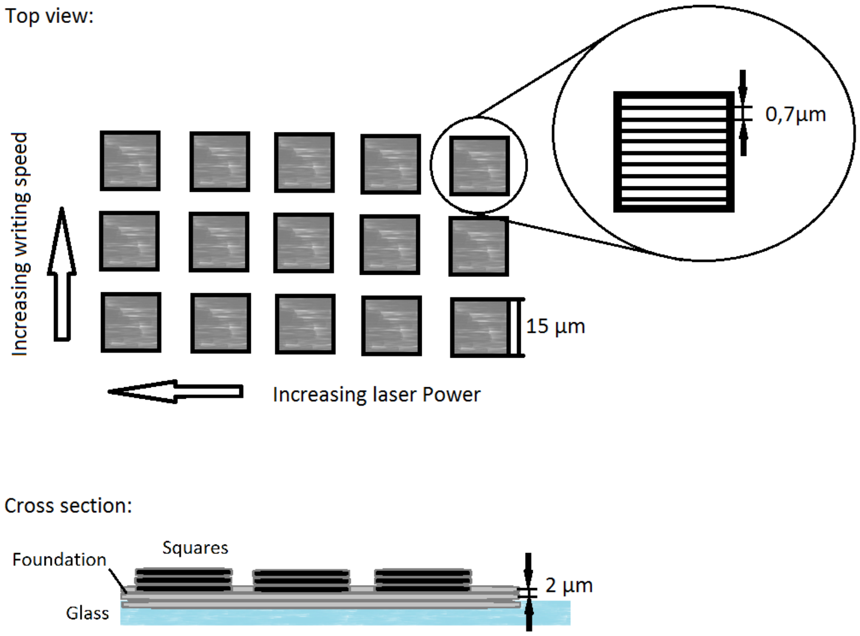

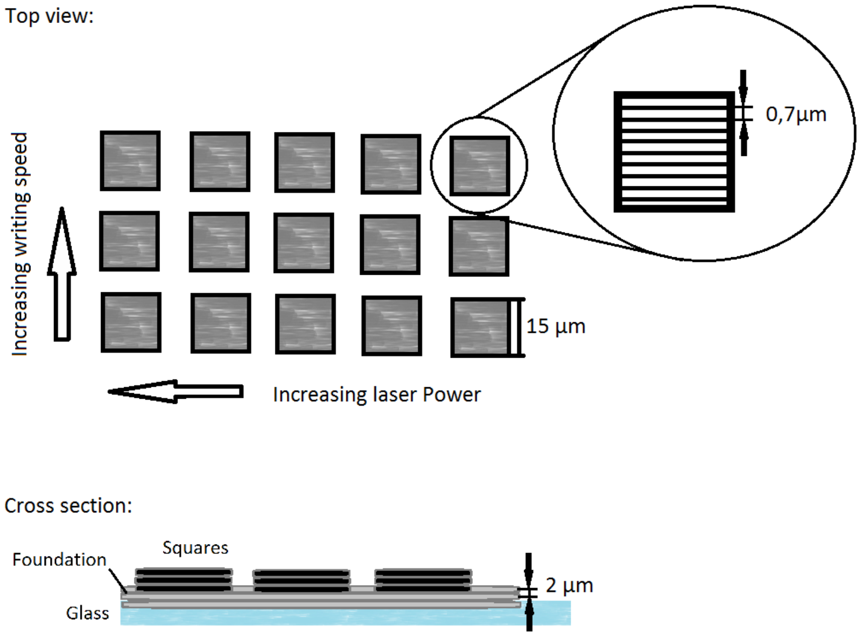

Figure 9 Schematical overview of experiment

In order to be sure that the squares are attached to the glass, a base layer was written as a fundament for the matrix, see Figure 9. This base layer consisting of three separate layers with a distance of 2 µm, also compensates for the fact that the sample can be under an angle with respect to the focus plane. By making sure the focus position is in the object glass while writing the first layer of the foundation, the whole base layer will be attached to the glass. The actual squares were also built out of multiple layers, of which the first layer is written into the top layer of the foundation, to be sure the squares are attached to it.

4 Results

After developing the samples, SEM pictures were taken in order to investigate the structure resulting from the various process settings that were used to create them. In this chapter the results of the experiments will be presented and compared to the theory given in paragraph 2.3.

4.1 PEGda600

For the PEGda 600 with both 1% and 0.5% Irgacure 369 there were no significant results that suggested writing by 2PP was possible at all. Though something looking like overpolymerization was observed on the in process camera for a laser power of 140 mW and above and velocities of 0.05 mm s^{-1} and below.

4.2 Irgacure 2959

Though some resins containing this photo initiator were tested, none of them produced any visible results. At near maximum power however, the in-process camera showed some bright flashes, which could be signs of a reaction taking place. The extinction spectrum of Irgacure 2959 provided by the supplier shows that it´s absorption at 395 nm is zero see Figure 4.

4.3 Varying water content

Though the original goal was to test the influence of varying the water content of the resin on the 2PP process, this could not be tested. At a certain point the Irgacure 369 reacted with the PEGda as soon as the two substances were mixed. After a few more tries with different PEGda and other photo initiators it was concluded that the Irgacure 369 had gone bad and could not be used anymore.

4.4 PEGda 700 with 1%^{wt} Irgacure 369

For PEGda 700 with 1%^{wt} of Irgacure 369, two successful experiments were carried out with different process parameters, see Table 5. All the samples presented are oriented like Figure 9, so with writing speed ranging from low speed at the bottom to high speed at the top of the picture and laser power ranging from high power on the left to low power on the right of the picture. Next to the SEM pictures a plot of the energy absorption by the resin due to 2PP is shown, calculated as described in paragraph 2.3. On the horizontal axis the angle of the halfwave plate is shown in order to scale the plot exactly the same as the corresponding SEM picture. The relation between this angle and the actual laser power is show in Figure 7.

Sample	Writing speed (mm/s)	Step size (mm/s)	Angle λ/2 plate (deg)	Step size (deg)	Power (mW)
27.5.no1 (low speed)	0.05-0.60	0.05	10-30	2	28.6 - 124.4
27.5.no1 (high speed)	1.00-1.95	0.05	0-20	2	77.0 – 148.1

Table 5 Process parameters for PEGda with 1%^{wt} Irgacure 369

The first test (27.5.no1 (low speed)) is shown in Figure 10. It is clearly visible that the foundation layer did not stick to the glass substrate, at the bottom left corner and at the top. The most important observations are the damaged structures at the bottom left of the matrix, where high power and low velocity are combined, and the fading structures to the upper left of the matrix, where low power and high speed are combined. The full power of the laser was not used, while it would most probably result in severe over polymerization and bubbles forming during the process, which could damage adjacent structures that would be undamaged otherwise.

The energy absorption plot is scaled logarithmically, because of the very large difference between the lowest and highest amount of absorbed energy. There seems to be some relation between the amount of energy absorbed by the resin due to the 2PP process and the resulting structures. The area with the damaged structures in the picture roughly corresponds to the area with an energy absorption of $10^{3.7}$ J cm^{-3} and higher (red-purple). And the area with the faint structures on the right side in the picture roughly corresponds to the area with an energy absorption of $10^{2.5}$ and lower in the graph (yellow-red). Except for some squares at the top-right that are somewhat less faint. The maximum absorbed energy per cubic centimetre is only 84 Joules, while the maximum lies at 19061 Joules per cubic centimetre.

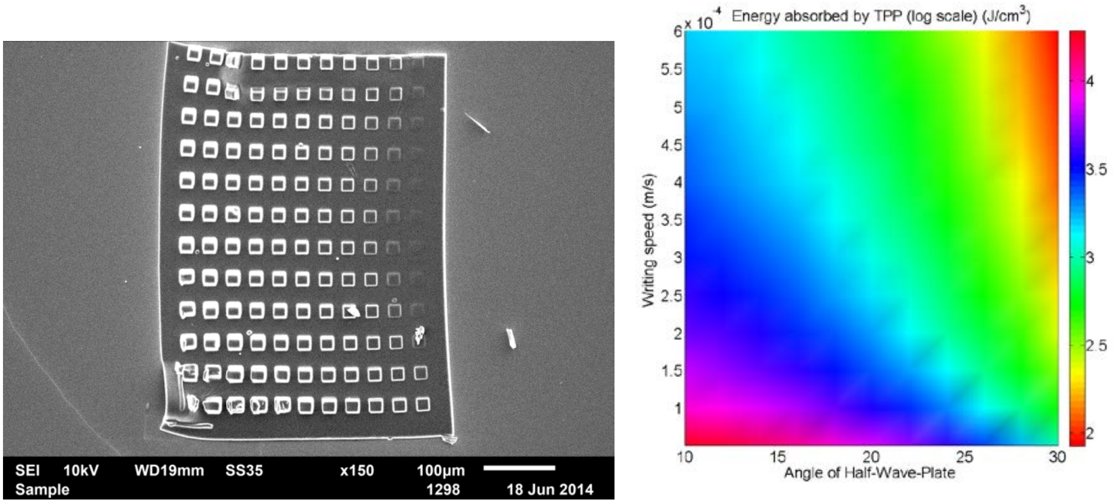

Figure 10 SEM picture of sample 27.05.no1 (low speed) and Energy absorption by 2PP plot velocity 0.05-0.60 mm s^{-1} power 28.6 - 124.4 mW

In the second experiment (27.5.no1 (high speed)) shown in Figure 11, higher velocities were used, which enable and even require the use of more power to give good results. Though no damaged structures can be seen at the bottom left part of the matrix, the structures again start fading with the use of higher writing speeds and lower power. In this experiment the minimum energy absorption was 187 J cm^{-3} while the maximum value is 1350 J cm^{-3}.

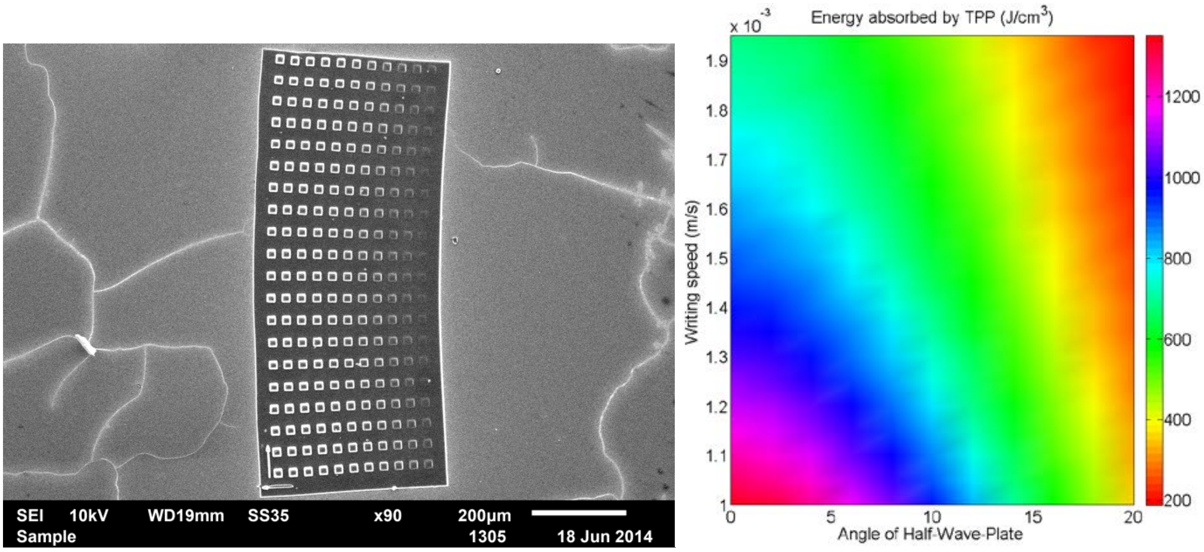

Figure 11 SEM picture of sample 27.05.no1 (high speed) and Energy absorption by 2PP plot velocity 1.00-1.95 mm s^{-1} power 77.0 – 148.1 mW

4.5 PEGda 700 with 0,5% Irgacure 369

In this paragraph the results for the second mixture are presented. The second mixture tested consisted of PEGda 700 (99.5%^{wt}) as a precursor and Irgacure 369 (0.5%^{wt}) as a photo initiator. For the process windows of each experiment see Table 6.

Sample	Writing speed (mm/s)	Step size (mm/s)	Angle λ/2 plate (deg)	Step size (deg)	Power (mW)
21.05.no1	0.04 – 0.56	0.04	4-30	2	28.6-142.7
02.06.no1	1.00 – 2.00	0.04	0-20	2	77,0 -148.1
02.06.no2	2.00 – 4.00	0.10	0-20	2	77,0 -148.1

Table 6 Process parameters for PEGda with 0.5%^{wt} Irgacure 369

In the first experiment (21.05.no1) shown in Figure 12, again relatively low speeds were tested. Again, the matrix shows some minor defects. Some squares are a little bit rotated, and at the edges the foundation seems not to be detached from the glass substrate.

The minimum value of absorbed energy lies at 90 J cm^{-3} while the maximum lies at 31339 J cm^{-3}. Though the photo initiator concentration is lower than in sample (27.05.no1(low speed)), see Figure 10, the maximum energy absorption is calculated to be higher because more laser power was used. As can be seen in paragraph 2.3, the amount of energy absorbed depends on the square of the laser power. In this experiment however, the qualitative relation between absorbed energy and the resulting structures is shown quite clearly. The area in the graph with energy absorption of 10$^{2.5}$ J cm^{-3} and below (yellow-red) corresponds to the area in the matrix where the squares are barely visible, whereas the region with energy absorption of 10^{4} and above (purple-red) corresponds to the bottom left area in the matrix where structures are over polymerized and damaged. The SEM picture and the energy absorption graph in Figure 12 show roughly the same iso-contours. Though it is hard to tell from Figure 12 which structures are damaged and which are not, when viewing the sample from a different angle, see Figure 13, it is easier to tell. Comparing this SEM picture with the energy absorbed at each position in the matrix, the damage threshold can be estimated. This energy absorption threshold above which structural damage starts to occur, seems to be around 4.5 10^{3} J cm^{-3} and 5.0 10^{3} J cm^{-3}.

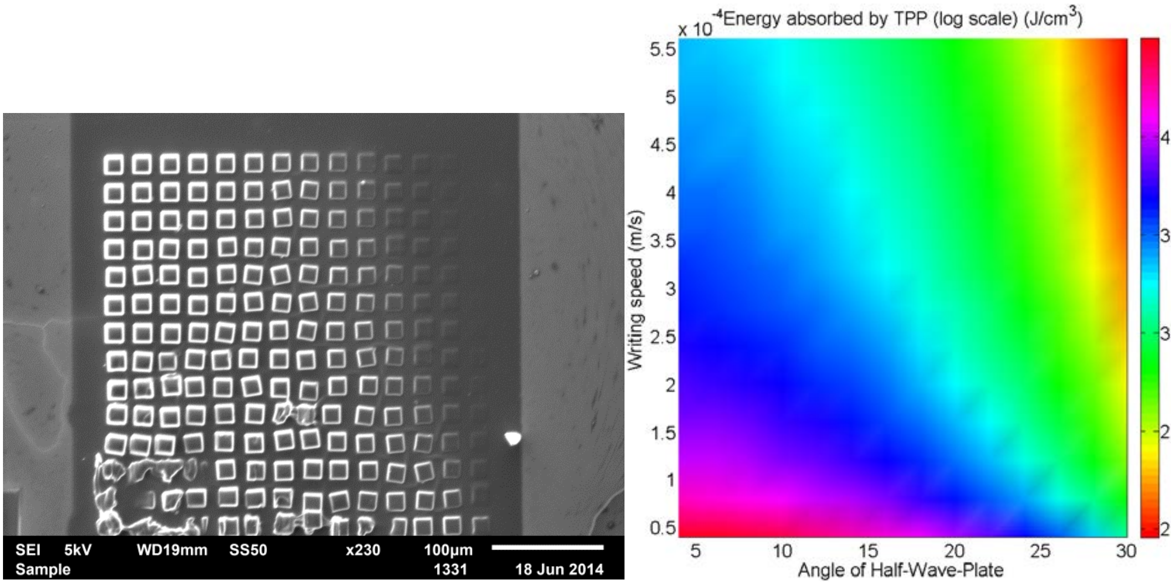

Figure 12 SEM picture of sample 21.05.no1 and Energy absorption by 2PP plot, velocity 0.04 – 0.56 mm s^{-1} power 28.6-142.7 mW

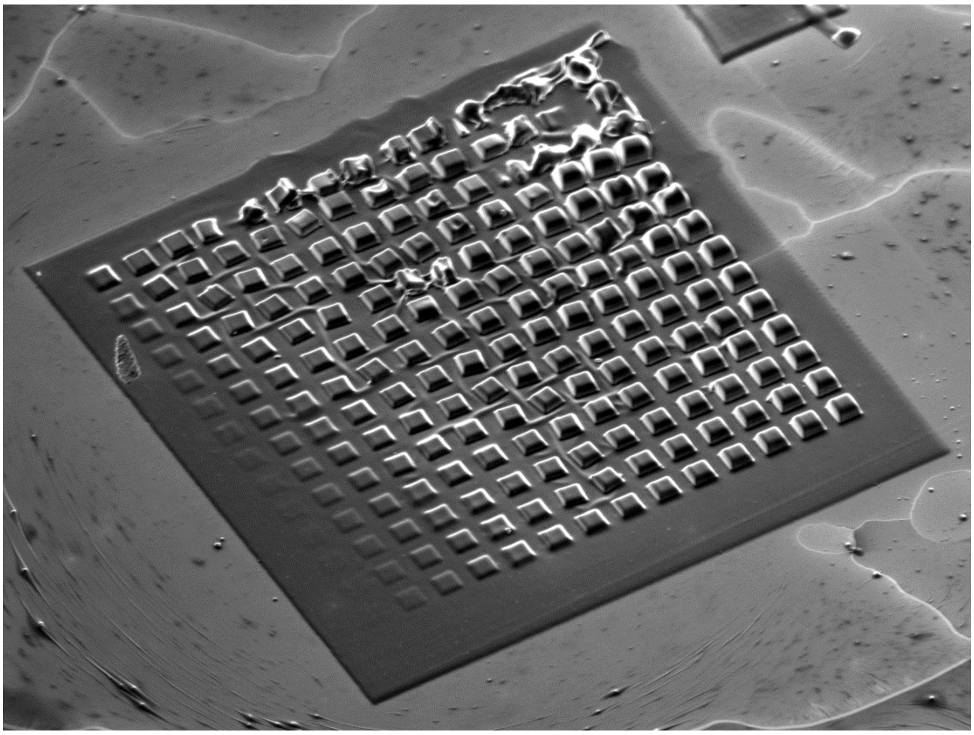

Figure 13 SEM picture of sample 21.05.no1 under a 45 degree angle, velocity 0.04 – 0.56 mm s^{-1} power 28.6-142.7 mW

In the second experiment (02.06.no1) conducted with this mixture higher laser power and writing velocity were tested as shown in Table 6. This time the matrix quality seems to be good, no places where the foundation is detached from the substrate and all the squares seem to be perfect in place.

The minimum energy absorption is 86 J cm^{-3} and the maximum value is 637 J cm^{-3}. Because the minimum writing speed in this experiment is about 50 times higher than in the first experiment, as shown in Table 6, the maximum energy absorption should be a factor 50 lower according to the calculation in paragraph 2.3. Again one can observe that the contour of the area with fading structures in the picture seems to correspond to the area with energy absorption of 200 J cm^{-3} and below (yellow red). In the bottom right corner an area with some brighter, higher structures is visible, of which the contour roughly corresponds with the contour of the area with an energy absorption of 550 J cm^{-3} and above in the graph.

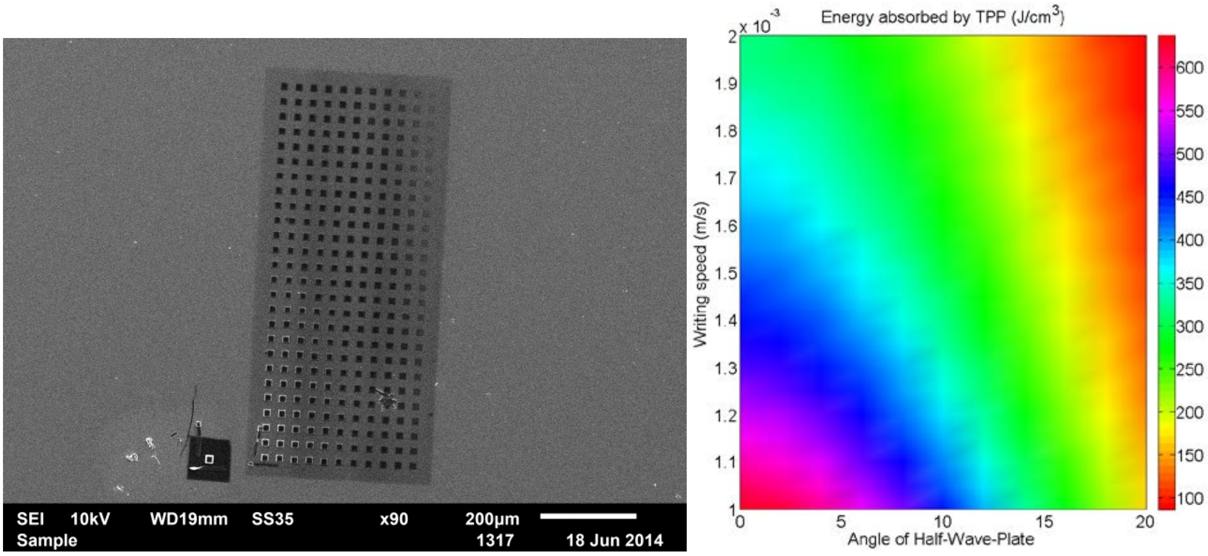

Figure 14 SEM picture of sample 02.06.no1 and Energy absorption by 2PP plot, velocity 1.00 – 2.00 mm s^{-1} power 77,0 -148.1 mW

In the third and last experiment (02.06.no2), conducted with the 0.5%^{wt} of photo initiator, even higher speeds were used, see Table 6. The results are shown in Figure 15. Except for something that could be a tear running through the matrix and a piece of debris that seems to be glass resulting from cutting the sample down to size, the matrix is of good quality (i.e. no detachments and all squares are in place).

The minimum and maximum energy absorption levels for this sample are 43 J cm^{-3} and 318 J cm^{-3} respectively. The difference between these levels of energy absorption and the levels observed in other experiments are again a consequence of the different process parameters and their relation to the absorbed energy as presented in paragraph 2.3. In the picture it is quite hard to see any difference between the structures, except for the more faint structures to the right. Under an angle of 45° see Figure 16, it is still hard to tell the difference between two adjacent structures. Since the maximum and minimum values of absorbed energy are close together, the difference between two adjacent squares is only very small. The only observation to be made is that the area with faint structures on the right of the matrix again shows correspondence to the area of low energy absorption (100 J cm^{-3} and below) in the graph.

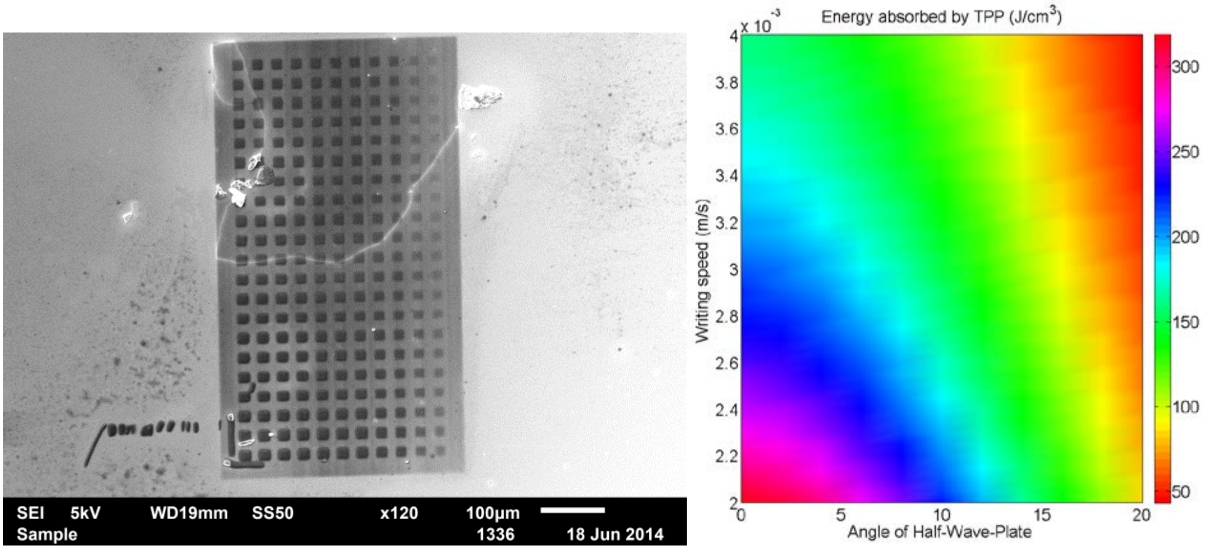

Figure 15 SEM picture of sample 02.06.no2 and Energy absorption by 2PP plot, velocity 2.00 – 4.00 mm s^{-1} power 77,0 -148.1 mW

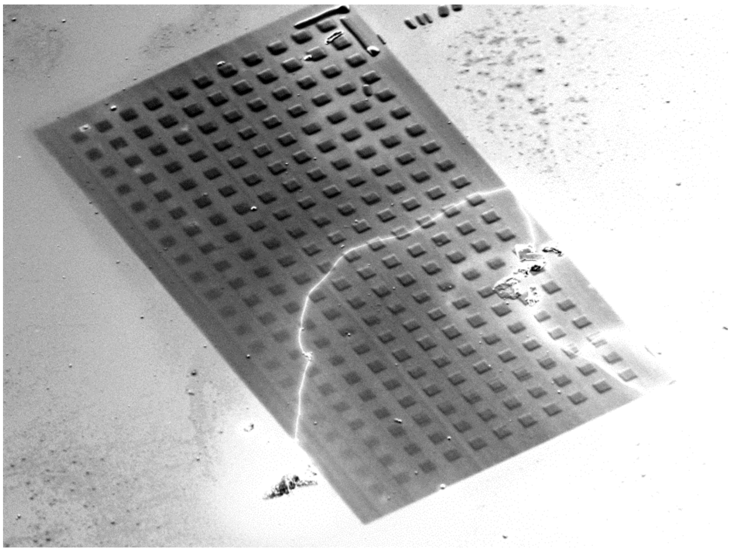

Figure 16 Sample 02.06.no2 viewed under an angle of 45˚, velocity 2.00 – 4.00 mm s^{-1} power 77,0 -148.1 mW

4.6 Self-organizing structures

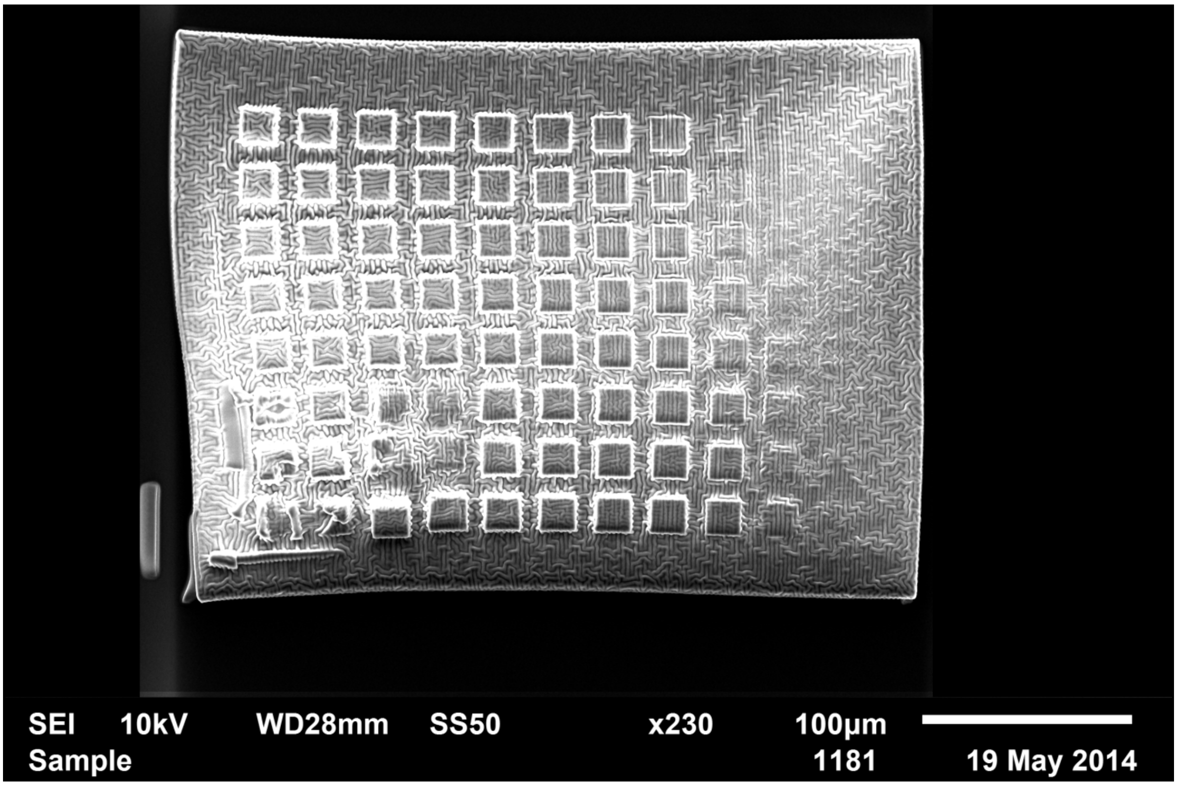

Figure 17 Test matrix PEGda velocity 0.12 – 0.40 mm/s, power 77,0 -148.1 mW

The result of one of the earlier experiments showed a remarkable pattern besides the expected matrix of squares, see Figure 17. One of the remarkable observations is that at some points the pattern follow the writing direction used in the experiment (i.e. bottom to top), while at other points it seems to be orientated perpendicular to this direction or even changing at will between the two directions. Though some attempt was made to analyse the periodicity and the orientation of the pattern with respect to the writing speed and power used. By taking the 2D fourier transform of sections the picture, as well as by calculating the autocorrelation of these same sections of the picture. Both methods did show promising results for larger areas of the picture. This sample however did not prove to be very well suited for such analyses. Each square made with a particular set of processing parameters only has a small area to be used for image processing, and as can be seen in Figure 17, the pictures suffer from some very strong relections from the perimeter of the squares. Due to the small area of each square these strong reflections are very likely of be of large influence on the results. The focus of this work is investigating the influence of different parameters on the process window, therefore no further effort was made to analyse these structures.

The damaged structures in the sample are caused by the problem of too low velocity at the beginning of writing each line, mentioned in paragraph 3.5.1.

5 Conclusions

Based on the results presented and the comparison with the calculations of the energy absorbed by the 2PP process, it can be concluded that there are signs of a direct relation between the absorbed energy and the height of the structures. Although it is not very clear from the experiments with 1% photo initiator, the experiments with 0.5%^{wt} photo initiator show more clear signs to support this conclusion.

Also there seems to be a threshold in the amount of absorbed energy below which 2PP can be realized without resulting in damaged structures, once this threshold is surpassed, by either using too much power or a too low speed, structural damage will occur. For the 1%^{wt} photo initiator mixture this threshold is a little hard to determine since it is not clear if the structures are damaged, or have changed form because the PEGda has the tendency to shrink when in dries. For the 0.5%^{wt} photo initiator resin, the results are a little more clear and the threshold seems to be somewhere between 4.5 10^3 J cm^{-3} and 5.0 10^3 J cm^{-3}.

As for the comparison between the different concentrations of photo initiators; as presented in paragraph 2.3 there is a linear relation between the concentration of photo initiator and the amount of energy absorbed. So a higher concentration of photo initiator leads to more energy absorption. At this time however there is no measurement data available to determine what the exact effect on the quality and dimension of the structures is. The only conclusion that can be drawn is that the resin with low photo initiator concentration seems to result in smaller structure heights (i.e. structures seem to be fading already at higher power and lower velocity) when compared to the resin with high photo initiator content.

6 Discussion and Outlook

The current experiments and measurements do not provide enough information to give a quantitative relation between the absorbed energy and the dimensions of the resulting structures. Therefore it would be interesting to make a height measurement of the samples and compare it with the amount of absorbed energy to quantify the relation between them.

Furthermore it would be of great value to know the dimension of the lines that result from writing at a certain velocity and with a certain power, this would help in optimizing the line distance and layer distance for minimizing production times. Since it is quite hard to measure the z-dimension of the written features directly, as they need to be attached to the glass somehow, an indirect approach would be easier. Such an indirect measurement can probably be measuring the width of the features in the xy-plane and calculating the power intensity around the focus position in 3-dimensions. With the assumption that the size of the created features corresponds to a volume in which a certain energy threshold is surpassed, the exact dimensions of the features can be deducted from the calculation.

Of course the influence of adding water to the mixture still have to be investigated as it can affect the quality of the resulting structures drastically. Not only will the concentrations of photo initiator and precursor be lower, but some other effects could be starting to occur. Water could get trapped in the created polymer network, and the consequences of this water evaporating for example, can be great. Furthermore the crosslink density of the structures, and thus their mechanical properties, could be affected greatly by adding water to the resin.

7 Publication bibliography

Birge, Robert R.; Pierce, Brian M. (1986): Semiclassical time-dependent theory of two-photon spectroscopy. The effect of dephasing in the virtual level on the two-photon excitation spectrum of isotachysterol. In *International Journal of Quantum Chemistry* 29 (4), pp. 639–656. Available online at http://dx.doi.org/10.1002/qua.560290407.

Ciba Specialty Chemicals Inc (2001a): Ciba Irgacure 369. Basel: Ciba Specialty Chemicals Inc.

Ciba Specialty Chemicals Inc (2001b): Irgacure 2959. 2001st ed.: Ciba Specialty Chemicals Inc, 2001.

Dr. ir. G.R.B.E. Römer (2009): Laser Materials Processing. Universiteit Twente.

Durst, Christopher A.; Cuchiara, Michael P.; Mansfield, Elizabeth G.; West, Jennifer L.; Grande-Allen, K. Jane (2011): Flexural characterization of cell encapsulated 5PEGDA6 hydrogels with applications for tissue engineered heart valves. In *Acta Biomaterialia* 7 (6), pp. 2467–2476. Available online at http://www.sciencedirect.com/science/article/pii/S1742706111000778.

Göppert-Mayer, Maria (1931): Über Elementarakte mit zwei Quantensprüngen. In *Annalen der Physik* 401 (3), pp. 273–294.

Hiroaki Nishiyama, Yoshinori Hirata, book - Lithography (2010): Femtosecond Laser Nonlinear Lithography. Available online at http://www.intechopen.com/books/export/citation/BibTex/lithography/femtosecond-laser-nonlinear-lithography.

Juodkazis, S.; Mizeikis, V.; Seet, K.K.; Miwa, M.; Misawa, H. (2005): Two-photon lithography of nanorods in SU-8 photoresist. In *Nanotechnology* 16 (6), pp. 846–849. Available online at http://www.scopus.com/inward/record.url?eid=2-s2.0-18744370446&partnerID=40&md5=4f1f27099a8629179ef25e554cb4b360.

Kaiser, W.; Garrett, C.G.B. (1961): Two-photon excitation in CaF2: Eu2+. In *Physical Review Letters* 7 (6), pp. 229–231. Available online at http://www.scopus.com/inward/record.url?eid=2-s2.0-26044464868&partnerID=40&md5=efba56e2a15860e1657e63e2c4f6567f.

Ovsianikov, A.; Chichkov, B.; Adunka, O.; Pillsbury, H.; Doraiswamy, A.; Narayan, R. J. (2007): Rapid prototyping of ossicular replacement prostheses. In *Applied Surface Science* 253 (15), pp. 6603–6607. Available online at http://www.sciencedirect.com/science/article/pii/S0169433207000669.

Panda, P.; Ali, S.; Lo, E.; Chung, B.G.; Hatton, T.A.; Khademhosseini, A.; Doyle, P.S. (2008): Stop-flow lithography to generate cell-laden microgel particles. In *Lab on a Chip - Miniaturisation for Chemistry and Biology* 8 (7), pp. 1056–1061. Available online at http://www.scopus.com/inward/record.url?eid=2-s2.0-46149093704&partnerID=40&md5=ae7e966f9fbd05416e55b3509f91eae2.

Pruzinsky, S. A.; Braun, P. V. (2005): Fabrication and Characterization of Two-Photon Polymerized Features in Colloidal Crystals. In *Advanced Functional Materials* 15 (12), pp. 1995–2004. Available online at http://dx.doi.org/10.1002/adfm.200500345.

Schafer, K.J.a; Hales, J.M.b; Balu, M.b; Belfield, K.D.a b b; van Stryland, E.W.b; Hagan, D.J.b (2004): Two-photon absorption cross-sections of common photoinitiators. In *Journal of Photochemistry and Photobiology A: Chemistry* 162 (2-3), pp. 497–502. Available online at http://www.scopus.com/inward/record.url?eid=2-s2.0-1342307566&partnerID=40&md5=2b269153fcbc380fb2d71ffa719f1901.

Xu, Chris; Webb, Watt W. (1996): Measurement of two-photon excitation cross sections of molecular fluorophores with data from 690 to 1050 nm. In *J. Opt. Soc. Am. B* 13 (3), pp. 481–491.

Appendix 1 Composition of investigated mixtures

Resin	H_2O (g)	Photo initiator	Quantity (g)	Precursor	Quantity (g)
I	2.13	Irgacure 2959	0.0296	PEGda 3460	0.891
II	1.203	Irgacure 2959	0.0310	PEGda 3460	1.785
III	1.163	Irgacure 2959	0.0297	PEGda700	1.749
IV	2.070	Irgacure 2959	0.0313	PEGda700	0.881
V	2.056	Irgacure 2959	0.0540	PEGda700	0.908
VI	-	Irgacure 2959	0.0292	PEGda600	2.970
VII	-	Irgacure 2959	0.0901	PEGda600	2.911
VIII	-	Irgacure 2959	0.0336	PEGda700	2.990
IX	-	Irgacure 2959	0.0907	PEGda700	2.987
X	-	Irgacure 369	0.0304	PEGda 600	2.970
XI	-	Irgacure 369	0.0309	PEGda 700	2.986
XII	-	Irgacure 369	0.0156	PEGda 600	2.988
XIII	-	Irgacure 369	0.0146	PEGda 700	3.007